JOURNAL OF GEOPHYSICAL RESEARCH, VOL. 93, NO. A9, PAGES 9893–9902, SEPTEMBER 1, 1988

An Investigation of the Second Negative System of O_2^+ by Electron Impact

G. K. JAMES,[1] J. M. AJELLO,[1] D. E. SHEMANSKY,[2] B. FRANKLIN,[1] D. SISKIND,[3] AND T. G. SLANGER[4]

We have measured the calibrated optically thin spectrum of O_2 from 115 to 300 nm induced by electron impact at 200 eV. Spectra were obtained in a crossed beam configuration at 1.25-nm resolution. We have observed the second negative system of O_2^+ ($A\ ^2\Pi_u \rightarrow X\ ^2\Pi_g$) in the range 186–300 nm. By comparison with O I (130.4 nm) and using the results of model calculations we estimate the emission cross section for the O_2^+ A state at 200 eV to be $2.57 \pm 0.57 \times 10^{-18}$ cm^2. The excitation function from threshold to 400 eV has also been measured at 220 nm and compared to the total ionization cross section. We have used the results of our laboratory measurements to model the contribution made by the second negative system of O_2^+ to auroral spectra in the same wavelength range. Observations of the spectral region from 140 to 185 nm show no detectable O or O^+ transitions with a cross section upper limit of 10^{-21} cm^2.

INTRODUCTION

As part of a continuing program established to measure absolute emission cross sections of atmospheric species excited by electron impact, we have obtained the calibrated optically thin fluorescence spectrum of the second negative system of O_2^+ ($A\ ^2\Pi_u \rightarrow X\ ^2\Pi_g$).

An overview of relevant electronic states and band systems of O_2 and O_2^+ is shown in Figure 1. *Krupenie* [1972] gives a comprehensive compilation of observed and predicted spectroscopic data on O_2 and its ions. Previous laboratory measurements of permitted transitions by electron impact include the first negative system of O_2^+ ($b\ ^4\Sigma_g^- \rightarrow a\ ^4\Pi_u$). Absolute excitation cross sections for the emission of this band system have been measured by *McConkey and Woolsey* [1969]; the peak cross section for the $b\ ^4\Sigma_g^-$ state was found to be 32.5×10^{-18} cm^2 at 100 eV. This band system has been observed in the aurora by several authors including *Gattinger and Vallance Jones* [1974] and has been discussed by *Chamberlain* [1961]. The upper state of the Schumann-Runge system of O_2 ($B\ ^3\Sigma_u^- \rightarrow X\ ^3\Sigma_g^-$) is almost completely predissociated and has not been seen in emission following electron impact, though electron scattering measurements have been performed by *Trajmar et al.* [1972] and *Wakiya* [1978*a*], who measured the differential and integral cross sections.

Observed forbidden transitions include the Herzberg I system of O_2 ($A\ ^3\Sigma_u^+ \rightarrow X\ ^3\Sigma_g^-$); differential and integral electron scattering cross sections for excitation of this system have been measured by *Trajmar et al.* [1972] and *Wakiya* [1978*b*]. However, the radiative lifetime of the A state is approximately 150 ms [*Klotz and Peyerimhoff*, 1986; *Saxon and Slanger*, 1986], which makes it difficult to see in emission. By comparison the lifetime of the $A\ ^2\Pi_u$ state of O_2^+ is approximately 660 ns [*Erman and Larsson*, 1977].

In addition, *Ajello and Franklin* [1985] have measured the EUV spectrum resulting from electron impact excitation of O_2 which consisted of a multitude of emission features in the wavelength range 40–130 nm due to dissociative excitation and dissociative ionization excitation processes.

The second negative system of O_2^+ ($A\ ^2\Pi_u \rightarrow X\ ^2\Pi_g$) has been extensively investigated in emission using discharge sources [see *Byrne*, 1961]. Electron impact studies have been made for the excitation of this system by *Stewart and Gabathuler* [1958], by *McConkey and Woolsey* [1969] at 100 eV electron energy, and by *Korol et al.* [1968] from threshold to 140 eV. However, these preliminary investigations only measured emission cross sections of a few individual vibrational transitions and did not contain model calculations. In addition, there were discrepancies in the measurements. For example, the cross section for the (2,5) transition at 100 eV was measured by Stewart and Gabathuler to be 5.9×10^{-20} cm^2; this compares to a value of 9×10^{-20} cm^2 obtained by McConkey and Woolsey.

In the present work we present emission spectra corresponding to the second negative system of O_2^+ obtained using a crossed-beam configuration under optically thin conditions over an extended wavelength range from the onset of this system at 185.9 to 300 nm. We have also performed model calculations to derive the total cross section for this system and assist in the interpretation of the spectrum. In addition, observations of the spectral region from 140 to 185 nm have been made to attempt to detect O or O^+ transitions reported by *Erdman and Zipf* [1986*a*].

EXPERIMENTAL APPARATUS

The experimental apparatus and VUV calibration techniques have been described in detail in earlier publications [*Ajello and Srivastava*, 1981; *Ajello et al.*, 1982, 1984]. In brief, the instrument consists of an electron impact emission chamber in tandem with a UV spectrometer. A magnetically collimated beam of electrons (10–500 eV) is crossed under optically thin conditions with a beam of gas formed by a capillary array. Emitted photons are observed at 90° using a commercial 0.2-m monochromator with an F-type photomultiplier detector. The optical system is capable of 0.5-nm resolution with 100-μm slit widths.

The relative sensitivity of the monochromator and detector in the range 200–300 nm was established using a 40-W deuterium arc lamp ultraviolet standard of spectral irradiance. At wavelengths less than 200 nm, calibration of the

[1]Jet Propulsion Laboratory, California Institute of Technology, Pasadena.
[2]Lunar and Planetary Laboratory, University of Arizona, Tucson.
[3]Laboratory for Atmospheric and Space Physics, University of Colorado, Boulder.
[4]Chemical Physics Laboratory, SRI International, Menlo Park, California.

Paper number 8A9527.
0148-0227/88/008A-9527$05.00

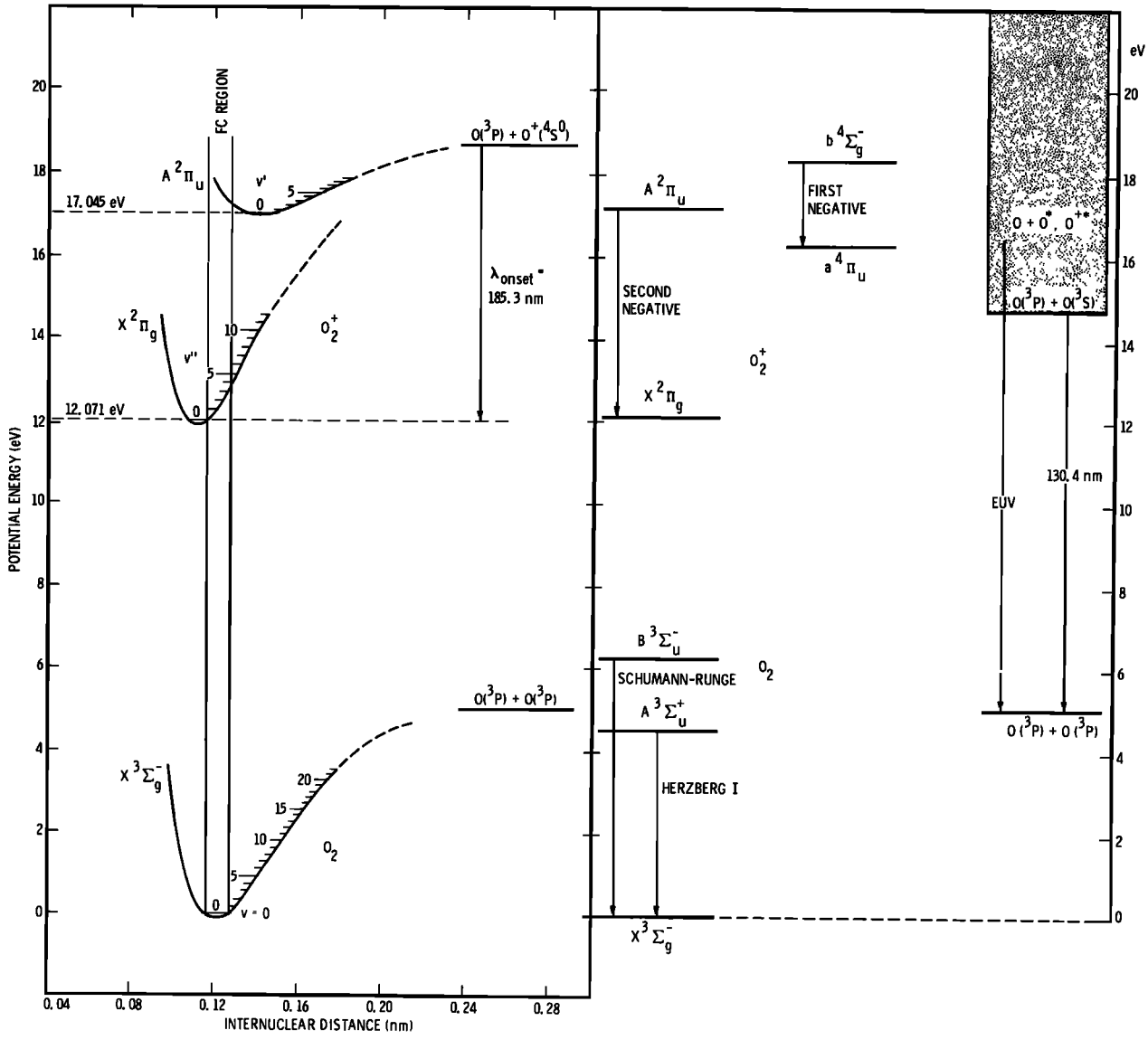

Fig. 1. Overview of the electronic states and band systems of O_2 and O_2^+.

optical system was performed using the molecular branching ratios for the Lyman-Birge-Hopfield (LBH) system of N_2 and H_2 Rydberg bands as described by *Ajello and Shemansky* [1985], *Shemansky et al.* [1985], and *Ajello et al.* [1988]. The relative accuracy of the calibration technique is 15%.

Spectral Data and Model

Figure 2 shows the calibrated optically thin emission spectrum from 115 to 300 nm induced by electron impact at 200 eV at a resolution of 1.25 nm. The spectrum was measured at a background gas pressure of 3.5×10^{-6} torr with a beam current of 200 μA. Clearly identifiable features in the FUV region are the allowed O I transitions at 115.2, 121.8, and 130.4 and the forbidden transition at 135.6 nm resulting from dissociative excitation of O_2, the most intense being the ^3P-^3S transition at 130.4 nm. It is interesting to note that the O I ^3P-^5S transition at 135.6 nm is observed even though it is relatively long lived ($\tau \approx 1.3$ ms).

The onset of the second negative band system of O_2^+ ($A\,^2\Pi_u \rightarrow X\,^2\Pi_g$) is clearly visible at 185.9 nm. This compares to the theoretical onset of 185.3 nm for a gas in thermal equilibrium at 300°K. To our knowledge this spectrum represents the first optically thin UV spectrum of O_2^+ induced by electron impact over this wavelength range.

The absolute cross section of O I (130.4 nm) used to normalize the entire VUV spectrum was determined by the relative flow technique developed in our laboratory [*Srivastava et al.*, 1975; *Trajmar and Register*, 1984]. In this method the Lyman α fluorescence signal at 200 eV electron impact energy from H_2, the standard gas, is compared to the fluorescence signal from O I (130.4 nm) emission produced by electron impact at 200 eV on O_2 at low background pressures in the molecular gas flow regime. The comparisons were made over a range of background gas pressures from 3×10^{-7} to 1×10^{-5} torr to establish linearity of signal with pressure. For the comparison of the signal strengths in the linear region, a value of 5.15×10^{-18} cm^2 was used as the cross section for Lyman α production by dissociative excitation of H_2 at 200 eV [*Pang et al.*, 1987]. By this method the cross section for O I (130.4 nm) at 200 eV was measured in

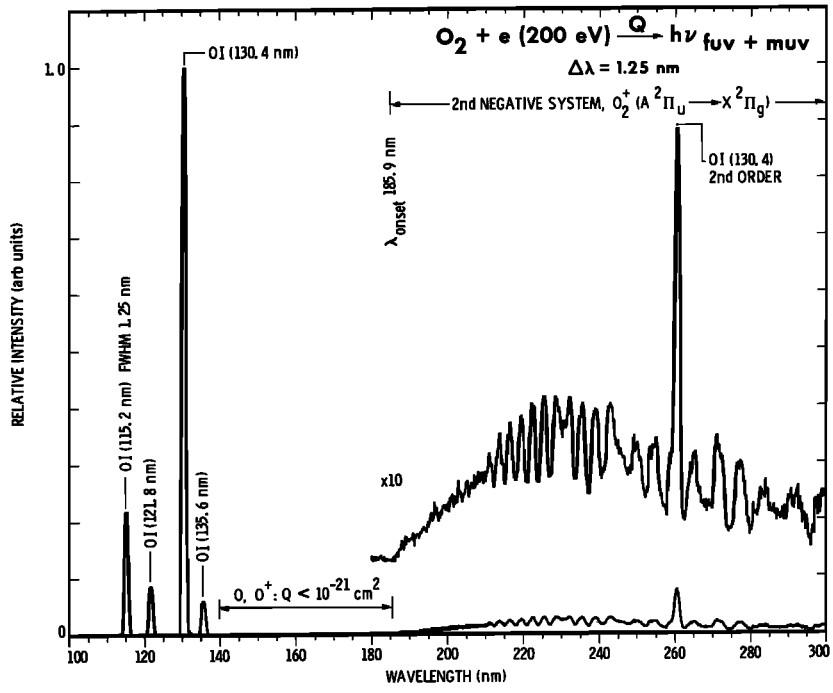

Fig. 2. Calibrated optically thin fluorescence spectrum of O_2 from 100 to 300 nm induced by electron impact at 200 eV with $\Delta\lambda$ = 1.25 nm. The second negative system of O_2^+ is identified in the range 186–300 nm.

an earlier publication [*Ajello and Franklin*, 1985] to be 2.36 × 10^{-18} cm^2. However, the value for the H_2 Lyman α cross section used was 5.78 × 10^{-18} cm^2 [*Shemansky et al.*, 1985]. The revised H_2 Lyman α cross section of *Pang et al.* [1987] yields a revised O I (130.4 nm) cross section of 2.1 × 10^{-18} cm^2 at 200 eV.

The cross section for the second negative band system of O_2^+ ($A\,^2\Pi_u \rightarrow X\,^2\Pi_g$) from 185.9 to 300 nm was determined by comparison with the known O I transition at 130.4 nm to be 1.84 × 10^{-18} cm^2 at 200 eV, making an allowance for O I features in second order. We judge that there is an 8% uncertainty in our corrected Lyman α cross section [*Pang et al.*, 1987] together with a 15% uncertainty in relative calibration. The signal statistics and repeatability of the measurements provide relative cross sections to 5% accuracy. The resultant root sum square 1σ uncertainty is 22% for the cross sections listed in this publication.

In order to model the experimental data and to obtain a value for the cross section of the entire second negative system (which extends well beyond 300 nm) we have generated a synthetic spectrum of the band system.

The relative vibrational band intensities from a single electronic state of most diatomic molecules excited by electron impact at low pressure can be accurately determined by Franck-Condon factors or transition probabilities. The relative intensity $I_{v'v''}$ of a band system at high impact energy can be written

$$I_{v'v''} = \frac{Q_{v'}}{Q}\frac{A_{v'v''}}{A_{v'}} \tag{1}$$

where $Q_{v'}$ and Q are excitation cross sections to level v' and to all levels respectively, $A_{v'v''}$ is the emission transition probability between levels v' and v'', and $A_{v'}$ is the total transition probability (emission + predissociation). $I_{v'v''}$ is normalized and sums to unity for a band system with negligible predissociation. In the Born limit,

$$\frac{Q_{v'}}{Q} = \frac{\lambda_{v'0}{}^3 A_{v'0}}{\Sigma\lambda_{v'0}{}^3 A_{v'0}} \tag{2}$$

where $\lambda_{v'0}$ is the wavelength of band (v', 0). If we assume that the electronic transition moment is constant, substituting (2) into (1) using the fact that $\lambda_{v'0}{}^3 A_{v'0} \propto q_{v'0}$ simplifies the expression for $I_{v'v''}$

TABLE 1. Calculated Franck-Condon Factors $q_{v'0}$ (v' = 0 to 25) for the Upward Excitation O_2^+ $A^2\Pi_u \leftarrow O_2$ $X\,^3\Sigma_g^-$

v'/v''	0
0	0.002813
1	0.012255
2	0.029112
3	0.050141
4	0.070268
5	0.085263
6	0.093107
7	0.093914
8	0.089143
9	0.080735
10	0.070507
11	0.059867
12	0.049749
13	0.040673
14	0.032855
15	0.026315
16	0.020956
17	0.016631
18	0.013176
19	0.010436
20	0.008270
21	0.006562
22	0.005211
23	0.004143
24	0.003294
25	0.002610

Upper state: O_2^+ $A\,^2\Pi_u$: ω_e = 898.2 cm^{-1}, $\omega_e x_e$ = 13.57 cm^{-1}.
Lower state: O_2 $X\,^3\Sigma_g^-$: ω_e = 1580.193 cm^{-1}, $\omega_e x_e$ = 11.981 cm^{-1}.

TABLE 2. Calculated Franck-Condon Factors $q_{v'v''}$ (v' = 0 to 25, v'' = 0 to 25) for the Second Negative System O_2^+ ($A\ ^2\Pi_u \rightarrow X\ ^2\Pi_g$)

v'/v''	0	1	2	3	4	5	6	7	8	9	10	11	12
0	0.000002	0.000029	0.000254	0.001428	0.005699	0.017184	0.040673	0.077474	0.120800	0.156023	0.168287	0.152391	0.116206
1	0.000013	0.000205	0.001544	0.007166	0.022801	0.052210	0.087444	0.105579	0.085966	0.037700	0.001938	0.015021	0.070343
2	0.000055	0.000777	0.004954	0.018844	0.046885	0.078054	0.083560	0.048404	0.006015	0.009126	0.054645	0.077945	0.044307
3	0.000171	0.002077	0.011174	0.034450	0.065177	0.073298	0.039613	0.002268	0.015767	0.055663	0.048820	0.006863	0.011326
4	0.000417	0.004398	0.019881	0.048971	0.067563	0.044536	0.004852	0.011247	0.047566	0.036978	0.001467	0.021119	0.054609
5	0.000860	0.007861	0.029685	0.057306	0.053937	0.014661	0.002940	0.036483	0.036932	0.002457	0.017766	0.045307	0.014705
6	0.001557	0.012331	0.038642	0.056952	0.032508	0.000578	0.020288	0.039339	0.008695	0.008347	0.038683	0.015630	0.004077
7	0.002543	0.017435	0.044975	0.048773	0.013181	0.003765	0.033573	0.021543	0.000491	0.028792	0.022939	0.000382	0.030301
8	0.003819	0.022652	0.047626	0.035984	0.002135	0.015301	0.032288	0.004298	0.012592	0.029844	0.002343	0.017029	0.027878
9	0.005350	0.027432	0.046446	0.022425	0.000293	0.025228	0.020584	0.000332	0.024890	0.014336	0.003199	0.028138	0.006283
10	0.007069	0.031313	0.042059	0.011142	0.004848	0.028294	0.007919	0.007382	0.025180	0.001686	0.016159	0.018706	0.000799
11	0.008890	0.033990	0.035541	0.003726	0.011777	0.024548	0.000863	0.016530	0.015902	0.001300	0.022845	0.004391	0.011890
12	0.010716	0.035336	0.028078	0.000371	0.017767	0.017038	0.000651	0.021044	0.005626	0.008871	0.018057	0.000153	0.020468
13	0.012450	0.035386	0.020705	0.000314	0.021040	0.009221	0.004862	0.019416	0.000367	0.015942	0.008325	0.005829	0.017609
14	0.014009	0.034303	0.014163	0.002370	0.021279	0.003428	0.010132	0.013853	0.000982	0.017715	0.001398	0.013172	0.008519
15	0.015326	0.032319	0.008868	0.005360	0.019112	0.000492	0.013989	0.007533	0.004993	0.014411	0.000213	0.015995	0.001515
16	0.016354	0.029699	0.004950	0.008358	0.015547	0.000108	0.015417	0.002747	0.009339	0.008857	0.003228	0.013545	0.000177
17	0.017066	0.026696	0.002330	0.010777	0.011552	0.001409	0.014578	0.000358	0.012042	0.003846	0.007353	0.008444	0.003083
18	0.017453	0.023535	0.000806	0.012343	0.007840	0.003451	0.012243	0.000116	0.012528	0.000847	0.010246	0.003647	0.007026
19	0.017520	0.020392	0.000121	0.013023	0.004813	0.005486	0.009286	0.001236	0.011219	0.000001	0.011043	0.000774	0.009624
20	0.017284	0.017399	0.000015	0.012930	0.002608	0.007061	0.006396	0.002883	0.008920	0.000672	0.010022	0.000003	0.010112
21	0.016773	0.014644	0.000259	0.012247	0.001182	0.007992	0.003988	0.004429	0.006384	0.002037	0.007983	0.000682	0.008876
22	0.016013	0.012171	0.000670	0.011169	0.000390	0.008280	0.002213	0.005534	0.004137	0.003415	0.005663	0.001977	0.006814
23	0.015038	0.010000	0.001112	0.009874	0.000055	0.008041	0.001056	0.006081	0.002405	0.004434	0.003622	0.003214	0.004625
24	0.013884	0.008128	0.001495	0.008502	0.000007	0.007431	0.000398	0.006108	0.001224	0.004976	0.002099	0.004001	0.002734
25	0.012566	0.006527	0.001764	0.007143	0.000107	0.006574	0.000090	0.005769	0.000536	0.004965	0.001030	0.004432	0.001523

v'/v''	13	14	15	16	17	18	19	20	21	22	23	24	25
0	0.074703	0.040456	0.018413	0.007018	0.002285	0.000752	0.000591	0.000924	0.000851	0.000510	0.000304	0.000209	0.002497
1	0.124706	0.140701	0.115813	0.073327	0.036010	0.012842	0.000862	0.001802	0.003726	0.002704	0.001343	0.000643	0.008476
2	0.002869	0.017547	0.080890	0.131205	0.131253	0.097198	0.057947	0.027628	0.011749	0.008181	0.002908	0.001616	0.016008
3	0.059723	0.065892	0.018702	0.003267	0.056340	0.110985	0.066484	0.001025	0.012895	0.014755	0.003656	0.003576	0.022237
4	0.026611	0.000512	0.041280	0.069572	0.026821	0.002502	0.079661	0.113571	0.043814	0.031361	0.004797	0.005482	0.025350
5	0.005293	0.046395	0.036624	0.000233	0.035216	0.081606	0.056272	0.023824	0.029218	0.031575	0.002196	0.007338	0.025830
6	0.039583	0.023514	0.001336	0.040838	0.039788	0.001891	0.005337	0.002747	0.041104	0.048222	0.003375	0.004008	0.023724
7	0.023283	0.000802	0.034867	0.025188	0.000823	0.030233	0.004605	0.039346	0.065351	0.058328	0.002077	0.001738	0.022266
8	0.000247	0.024940	0.024757	0.000540	0.033089	0.014035	0.021002	0.093295	0.067101	0.055222	0.000953	0.000001	0.020069
9	0.011561	0.028048	0.000510	0.024513	0.021561	0.005151	0.071163	0.066165	0.055434	0.052725	0.001053	0.002525	0.018358
10	0.025573	0.007334	0.010823	0.026845	0.000038	0.038695	0.044768	0.022516	0.050051	0.054754	0.001600	0.008676	0.017370
11	0.019120	0.000529	0.024706	0.005873	0.013751	0.034468	0.005738	0.008606	0.053004	0.056829	0.001836	0.014739	0.016324
12	0.004991	0.011193	0.017565	0.001156	0.025097	0.007201	0.000614	0.012081	0.057635	0.055202	0.001746	0.018865	0.014666
13	0.000073	0.019503	0.003749	0.012665	0.014426	0.000681	0.001741	0.027239	0.057642	0.050284	0.001801	0.020646	0.012360
14	0.005418	0.016127	0.000366	0.018926	0.001642	0.008655	0.000076	0.045527	0.051828	0.044519	0.002329	0.020092	0.009635
15	0.012528	0.007026	0.006658	0.013320	0.001584	0.010349	0.007089	0.053395	0.043126	0.039654	0.003485	0.017654	0.006790
16	0.014944	0.000832	0.013101	0.004295	0.009047	0.004337	0.021847	0.047282	0.034813	0.036074	0.005261	0.014221	0.004150
17	0.012133	0.000529	0.013969	0.000069	0.013731	0.000085	0.032721	0.034047	0.028483	0.033366	0.007467	0.010736	0.002027
18	0.007030	0.003956	0.010038	0.001721	0.012125	0.002213	0.033011	0.021437	0.024242	0.030943	0.009818	0.007816	0.000636
19	0.002630	0.007678	0.004882	0.005810	0.007026	0.008070	0.025096	0.012848	0.021539	0.028389	0.012049	0.005668	0.000038
20	0.000351	0.009568	0.001263	0.008915	0.002396	0.013044	0.014947	0.008111	0.019718	0.025547	0.013962	0.004222	0.000125
21	0.000099	0.009319	0.000012	0.009610	0.000186	0.014708	0.006911	0.005923	0.018270	0.022482	0.015432	0.003304	0.000678
22	0.001049	0.007581	0.000546	0.008371	0.000268	0.013179	0.002274	0.005163	0.016849	0.019345	0.016379	0.002738	0.001443
23	0.002350	0.005383	0.001827	0.006071	0.001572	0.010062	0.000380	0.005171	0.015322	0.016315	0.016761	0.002388	0.002197
24	0.003518	0.003470	0.002970	0.003725	0.003100	0.006863	0.000000	0.005577	0.013671	0.013537	0.016594	0.002157	0.002786
25	0.003958	0.001805	0.003911	0.002166	0.003757	0.003631	0.000239	0.005711	0.011838	0.011013	0.015839	0.001974	0.003130

Upper state: O_2^+ $A\ ^2\Pi_u$: ω_e = 898.2 cm^{-1}, $\omega_e x_e$ = 13.57 cm^{-1}. Lower state: O_2^+ $X\ ^2\Pi_g$: ω_e = 1904.7 cm^{-1}, $\omega_e x_e$ = 16.25 cm^{-1}.

$$I_{v'v''} = \frac{q_{v'0}A_{v'v''}}{A_{v'}} = q_{v'0}\frac{q_{v'v''}/\lambda_{v'v''}^3}{\sum_{v''}(q_{v'v''}/\lambda_{v'v''}^3)} \quad (3)$$

where $q_{v'v''}$ is the Franck-Condon factor between vibrational levels v' and v''.

Thus we can use Franck-Condon factors to compute transition probabilities and hence the intensity for each vibrational transition. The output of this calculation is then convolved with the instrumental slit function to generate a synthetic spectrum at the same resolution as the experimental data.

Using the Morse potential, we have calculated Franck-Condon factors $q_{v'0}$ (v' = 0 to 25) for the upward excitation O_2^+ $A\ ^2\Pi_u \leftarrow O_2$ $X\ ^3\Sigma_g^-$ and $q_{v'v''}$ (v' = 0 to 25, v'' = 0 to 25) for the second negative system of O_2^+ ($A\ ^2\Pi_u \rightarrow X\ ^2\Pi_g$). These are listed in Tables 1 and 2 together with the molecular constants used in the calculation. This represents a considerable extension of previously available Franck-Condon factors for this system. *Krupenie* [1972] lists $q_{v'v''}$ for the second negative system of O_2^+ for v' = 0 to 8, v'' = 0 to 10, and *Wacks* [1964] has calculated $q_{v'0}$ O_2^+ $A\ ^2\Pi_u \leftarrow O_2$ $X\ ^3\Sigma_g^-$ for v' = 0 to 20. There is good agreement between our calculated Franck-Condon factors and both these other sets of data.

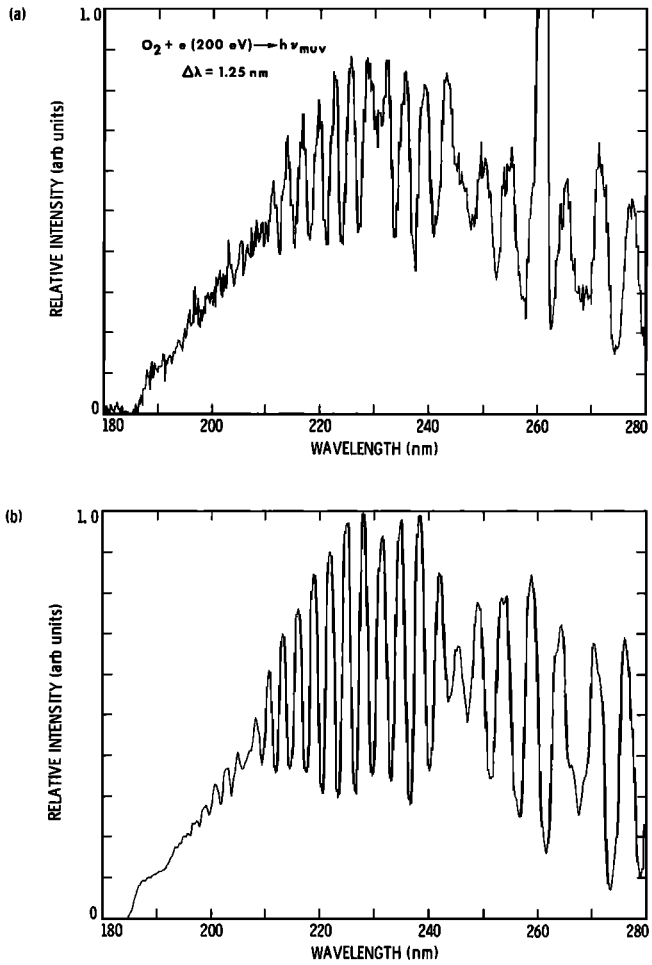

Fig. 3. Comparison of the experimental and synthetic spectra of the O_2^+ (A-X) system in the range 180–280 nm at a resolution of 1.25 nm. (*a*) UV emission spectrum $O_2 + e$ (200 eV) → O_2^+ (A-X). (*b*) Synthetic spectrum O_2^+ (A-X).

TABLE 3. Summary of Cross-Section Measurements Used in This Work

	Q, × 10^{-18} cm^2	Energy, eV	Reference
121.6 nm H_2 Lyman α	5.15	200	*Pang et al.* [1987]*
130.4 nm O I	2.1	200	this work*
117.26 nm O I	<0.001	100	this work*
O_2^+ second negative system	2.57	200	this work*
O_2^+ first negative system	32.5	100	*McConkey and Woolsey* [1969]
O_2 total ionization	253	200	*Rapp and Englander-Golden* [1965]

*Values are ±22%.

transition moment is a linear function with a small gradient (maximum variation ±15%) with the r-centroid in the range 0.12–0.15 nm.

2. We have assumed that predissociation is negligible.

3. The Morse potential method for calculating Franck-Condon factors is inherently inaccurate for high v'. This may be an important source of error in the model especially since the data possibly contain significant contribution from high v' components. However, comparison with Franck-Condon factors calculated using the RKR method [*Krupenie*, 1972; D. C. Cartwright, private communication, 1987] shows agreement to within approximately 10% up to v' of 10.

In addition, the effect of rotational structure on the spectrum needs to be considered in the model calculations. The O_2^+ (A-X) transition shows intermediate coupling between Hund's case a and case b. The upper $A\ ^2\Pi_u$ state is close to case b, but the ground $X\ ^2\Pi_g$ state shows relatively large spin-orbit splitting (A approximately 200 cm^{-1}). As a consequence, the transition has 12 branches. The four Q branches

The main limitations of this model are as follows:

1. We have assumed a constant electronic transition moment. However, this is not expected to have a large effect. *Erman and Larsson* [1977] used the results of lifetime measurements to deduce that the variation of electronic

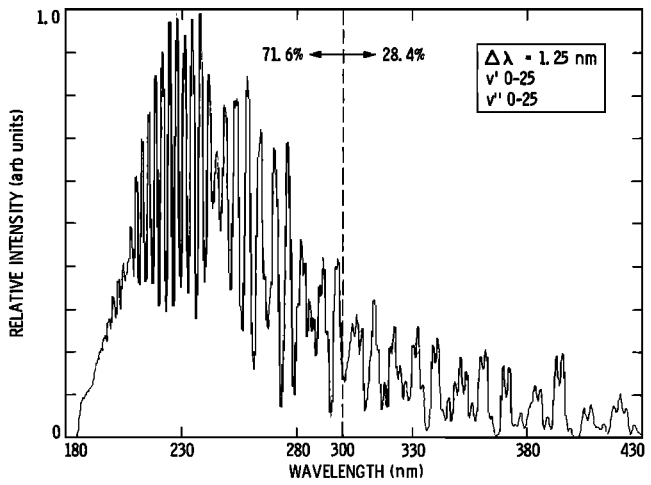

Fig. 4. Synthetic spectrum of the second negative system O_2^+ ($A\ ^2\Pi_u \rightarrow X\ ^2\Pi_g$) for $v' = 0$ to 25, $v'' = 0$ to 25, and $\Delta\lambda = 1.25$ nm.

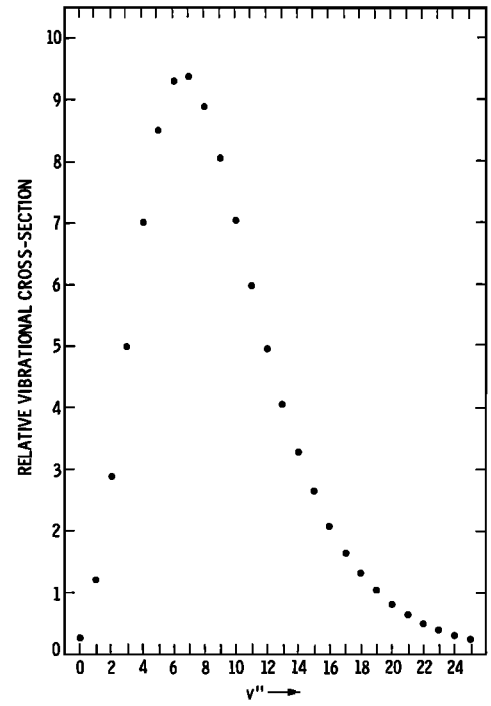

Fig. 5. Relative vibrational excitation cross section $O_2^+\ A\ ^2\Pi_u \leftarrow O_2\ X\ ^3\Sigma_g^-$ as represented by $q_{v'0}$ for $v' = 0$ to 25.

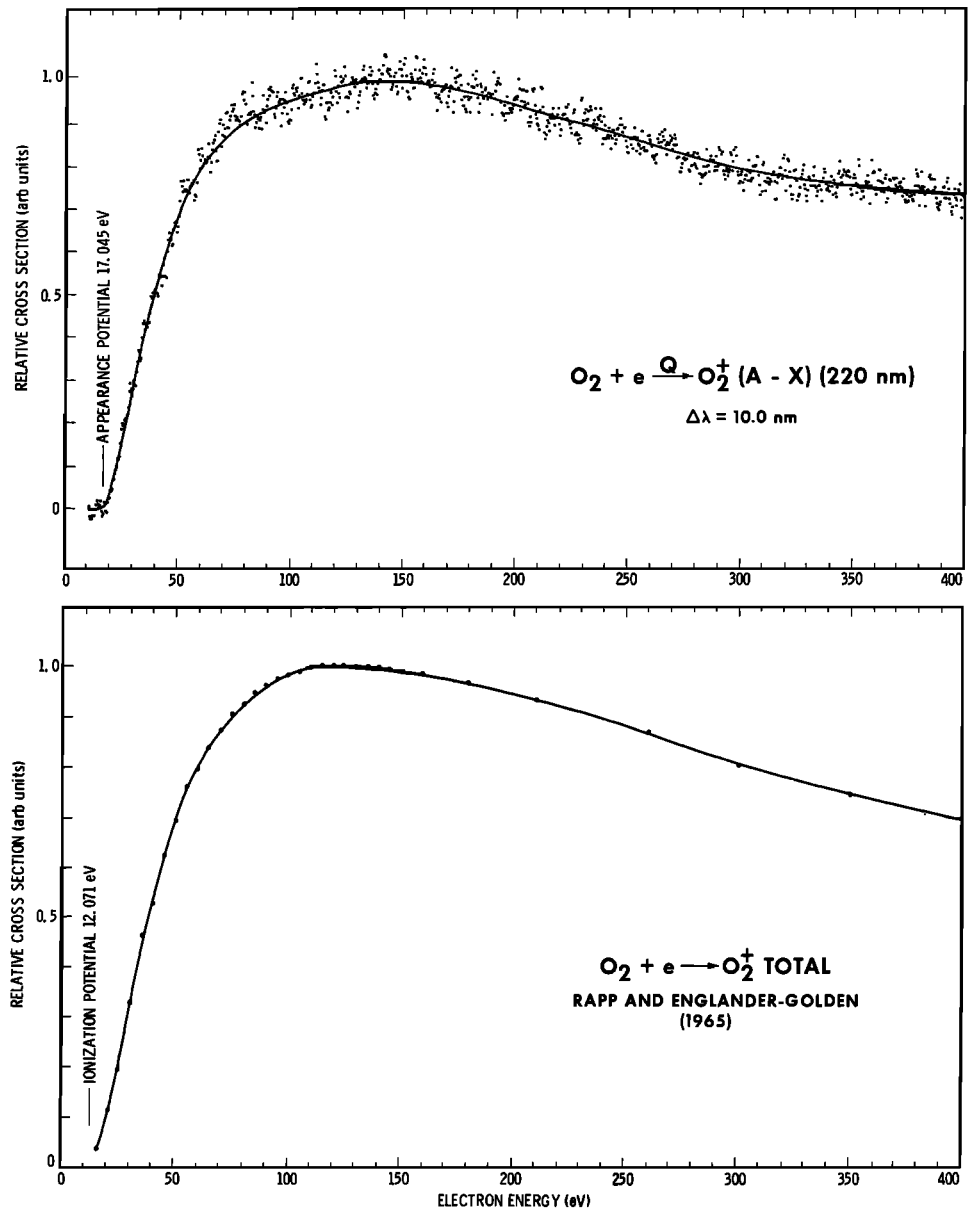

Fig. 6. Relative emission cross section for the second negative system O_2^+ ($A\ ^2\Pi_u \rightarrow X\ ^2\Pi_g$) at 220 nm from threshold to 400 eV at a resolution of 10 nm.

are relatively weak, but the remaining R and P branches have comparable intensities at 300°K. The small splitting of the $A\ ^2\Pi_u$ state results in the production of two sets of six branches separated essentially by the spin-orbit splitting of the $X\ ^2\Pi_g$ state (approximately 200 cm^{-1}). A fully developed fine structure model for the O_2^+ (A-X) transition has not been developed for the current work. The model shown in Figure 3 in comparison with the data has been constructed using P_{22} (9.5), P_{11} (9.5), R_{22} (7.5), and R_{11} (7.5) rotational transitions of equal intensity to represent the entire band. This relatively crude model appears to fit the data with acceptable accuracy. Constants for the system have been most recently determined by *Coxon and Haley* [1984] [cf. *Huber and Herzberg*, 1979]. High vibrational level coupling constants were obtained by extrapolating the data of *Coxon and Haley* [1984] for $v'' > 12$ and $v' > 15$. Rotational line strength factors for intermediate coupling are not explicitly formulated in the published literature but can be derived from general formulae given by *Hill and Van Vleck* [1928].

The complete synthetic spectrum of O_2^+ ($A\ ^2\Pi_u \rightarrow X\ ^2\Pi_g$) is shown in Figure 4 at a resolution of 1.25 nm. Approximately 72% of the band system lies in the range of our experimental spectrum at wavelengths below 300 nm. This enables us to estimate the cross section for the entire second negative system at 200 eV to be $2.57 \pm 0.57 \times 10^{-18}$ cm^2 based on our experimental value of 1.84×10^{-18} cm^2 for the region below 300 nm. A summary of cross section measurements used in this work is given in Table 3.

The relative vibrational excitation cross section as represented by the calculated Franck-Condon factors $q_{v'0}$ as a function of v' for the upward transition O_2^+ $A\ ^2\Pi_u \leftarrow O_2$ $X\ ^3\Sigma_g^-$ is plotted in Figure 5 for $v' = 0$ to 25. This function peaks at $v' = 7$ showing the importance of including higher v' in the model.

In an attempt to explain intensity anomalies observed in the relative direct excitation cross section of O_2^+ $A\ ^2\Pi_u$ by *Lin et al.* [1987] it was suggested that the lowest-v' vibrational levels are populated mainly by cascade from higher

states, possibly O_2^+ $B\ ^2\Sigma_g^-$. The $^2\Sigma_g^-$ state lies in the correct energy region of the potential energy curves of O_2^+ [*Krupenie*, 1972] and excitation of $^2\Sigma_g^-$ has been observed by both the convergence of a Rydberg series [*Yoshino and Tanaka*, 1968] and by photoelectron measurements [see *Edqvist et al.*, 1970]. However, radiation corresponding to the allowed transition O_2^+ ($B\ ^2\Sigma_g^- \rightarrow A\ ^2\Pi_u$) has not been observed. *Doolittle et al.* [1968] studying photoionization of O_2 with 58.4–35.8 nm photons have observed possible predissociation of O_2^+ $B\ ^2\Sigma_g^-$. Predissociation lifetime, short relative to the radiative lifetime which was estimated as 10^{-8}s, was assumed to explain the absence of this allowed transition.

We have also measured the excitation function for the O_2^+ second negative system from 0 to 400 eV at 220 nm with 10-nm resolution. The excitation function shown in Figure 6 can be put on an absolute scale by normalizing to the cross section measured from our spectrum at 200 eV. Absolute emission cross sections for the second negative system from 17.5 to 400 eV are listed in Table 4. The energy scale was calibrated by measuring the appearance potential (21.2 eV) of the 58.4-nm He line. The theoretical appearance potential of 17.045 eV for this band system is consistent with our experimental value which was reproducible to ±0.5 eV and supports the identification of this band system (see Figure 1). Also shown in Figure 6 is the total ionization cross section measurement of *Rapp and Englander-Golden* [1965]. It is interesting to note the similarity in the shape of the two excitation functions. Excitation to the $A\ ^2\Pi_u$ state of O_2^+ proceeds mainly via direct ionization of a π_u valence electron from the ground state of O_2 to give rise to the second negative system. The ratio of the two cross sections is approximately 2 orders of magnitude.

Erdman and Zipf [1986*a*] have recently published electron impact induced fluorescence spectra of O_2 at 100 eV. They have carefully measured a spectral line at 164.13 nm, which arises from the transition O I (^1D–^3S). As direct evidence for this weak emission, Erdman and Zipf have shown electron impact spectra at 0.2- and 0.017-nm resolution from 130 to 170 nm produced at a background pressure of 5×10^{-4} torr by an intense electron beam current of 2 mA. The spectra of Erdman and Zipf show a host of line emissions for which wavelength identifications are not given. The line emissions have been tentatively identified as uncatalogued O^+ lines because of their energy dependence. We suggest that impurity gases are the more likely sources of these spurious emissions.

In Figure 7 we compare electron impact-induced fluorescence spectra measured by the two laboratories. It is clear that our spectrum shows no unexpected features arising from uncatalogued O^+ of cross section larger than 10^{-21} cm^2. Counting statistics for our measurement are described in Figure 7. Research grade O_2 contains many residual gases (N_2, CO, CO_2, A, Kr, Xe, N_2O, H_2, CH_4) present at a concentration level of 10^{-5} to 10^{-7}. For example, the strong impurity emissions observed by Erdman and Zipf at approximately 139.9, 159.4, and 165.2 nm can be tentatively identified as bands in the fourth positive system of CO from electron impact of CO and CO_2 [*Ajello*, 1971*a*, *b*]. Additionally, electron bombardment of lens elements can yield metallic ions. This level of concentration would produce apparent cross sections for O_2 of 10^{-22} to 10^{-24} cm^2, particularly from resonance lines.

TABLE 4. Absolute Emission Cross Sections for the Second Negative System O_2^+ ($A\ ^2\Pi_u \rightarrow X\ ^2\Pi_g$) From 17.5 to 400 eV Measured From Data in Figure 6

Energy, eV	Absolute Cross Section, 10^{-18} cm^2
17.5	0.01
20.0	0.08
22.5	0.24
25.0	0.45
27.5	0.61
30.0	0.76
32.5	0.90
35.0	1.10
37.5	1.22
40.0	1.36
42.5	1.44
45.0	1.58
47.5	1.70
50.0	1.84
52.5	2.01
55.0	2.03
57.5	2.03
60.0	2.19
62.5	2.19
65.0	2.23
67.5	2.29
70.0	2.37
72.5	2.44
75.0	2.47
77.5	2.49
80.0	2.50
82.5	2.52
85.0	2.42
87.5	2.47
90.0	2.58
92.5	2.53
95.0	2.52
97.5	2.52
100.0	2.51
102.5	2.59
105.0	2.59
107.5	2.59
110.0	2.58
112.5	2.64
115.0	2.56
117.5	2.53
120.0	2.63
122.5	2.64
125.0	2.61
127.5	2.64
130.0	2.59
132.5	2.71
135.0	2.70
137.5	2.59
140.0	2.70
142.5	2.78
145.0	2.67
147.5	2.65
160.0	2.67
180.0	2.59
200.0	2.57*
220.0	2.42
240.0	2.39
260.0	2.28
280.0	2.17
300.0	2.12
320.0	2.05
340.0	2.04
360.0	2.03
380.0	1.99
400.0	1.91

All tabulated values are ±22%.
*Normalization point at 200 eV: $Q = 2.57 \times 10^{-18}$ cm^2.

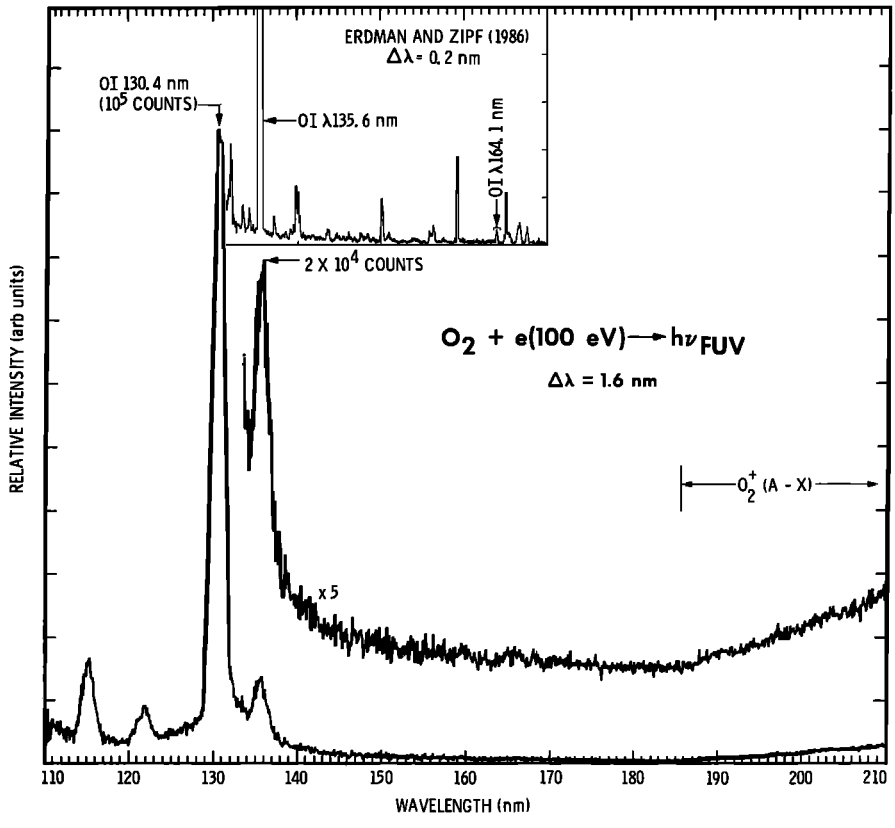

Fig. 7. Comparison of O_2 + e (100 eV) electron impact induced fluorescence from this work and that of *Erdman and Zipf* [1986*a*]. The spectrum obtained in this work was measured at 5×10^{-6} torr background gas pressure in a crossed beam configuration with an electron beam of 150 μA at a spectral resolution of 1.6 nm. The Erdman and Zipf spectrum was measured at 0.2-nm resolution. The total counts under 130.4 nm is 10^5, which has a cross section of 2.1×10^{-18} cm^2 as measured by our laboratory. The measurement limit of 50 counts for a spectral line in this particular experiment corresponds to an emission cross section of 10^{-21} cm^2.

The stronger impurity lines of Erdman and Zipf shown in Figure 7 are nominally 10^{-22} cm^2 based on a cross section of 1.22×10^{-23} cm^2 for the highlighted (Figure 7) 164.13-nm feature. Although this cross section value is smaller than our experimental upper limit (10^{-21} cm^2), our theoretical model of the O^+ energy levels shows no transitions in this spectral region are possible.

It is also interesting to note in Figure 7 the absence of any emission line at 117.26 nm in our spectrum corresponding to the O I transition $2p^4\ ^1D\text{-}3s'\ ^3D$. This enables us to establish an upper limit of 10^{-21} cm^2 for the cross section of this transition. This is consistent with the cross section value of $\sim 1.56 \times 10^{-22}$ cm^2 ($\pm 30\%$) obtained by *Erdman and Zipf* [1986*b*].

Application to Auroral Spectra

In recent years, ultraviolet spectra of the aurora between 110 and 290 nm have been studied by a number of authors [e.g., *Beiting and Feldman*, 1979; *Huffman et al.*, 1980; *Siskind and Barth*, 1987]. We have used the results of our laboratory measurements to model the contribution made by the second negative system of O_2^+ to auroral spectra in this wavelength range.

Using the excitation function shown in Figure 6, we have calculated the O_2^+ second negative emission rate in an aurora. The auroral electron fluxes for a 1 erg cm^{-2} s^{-1}, E_0 = 2 keV aurora were calculated using the computer model of D. J. Strickland (see, e.g., *Strickland et al.* [1983]). The volume production rate is given by

$$P(z) = n(z) \int_W \sigma(E)\phi(z, E)\, dE = n(z)g(z) \qquad (4)$$

where $n(z)$, the neutral density, is from the MSIS-83 (Mass Spectrometer/Incoherent Scatter) model atmosphere [*Hedin*, 1983], W is the excitation threshold, $\sigma(E)$ is the cross section, $\phi(z,E)$ is the flux, and $g(z)$, the g factor, is the excitation rate (s^{-1}). The results of this calculation are shown in Figure 8. For comparison the production rate of the N_2^+ (0,0) first negative band (N_2^+ 391.4 nm) is also shown. The ratio of the O_2^+ second negative system to N_2^+ 391.4 nm is approximately 1:40 at the lowest altitudes (a factor of 8 from the ratio of the g factors and a factor of 5 from the O_2/N_2 density ratio) and is largely independent of both the auroral characteristic energy and total flux. (This ratio is a factor of 20 smaller than that predicted by *Rees and Jones* [1973], who used the semiempirical cross sections of *Watson et al.* [1967].) Since O_2 has a slightly smaller-scale height than N_2, the O_2/N_2 ratio decreases with increasing altitude, and the emission ratio decreases to 1:100 for z = 200 km.

Using the above production rate, we have produced a model auroral spectrum containing the O_2^+ second negative bands. The maximum emission of the O_2^+ second negative system occurs in the 200- to 240-nm region where the strongest nitrogen emissions are from the Lyman-Birge-Hopfield (LBH) and the Vegard-Kaplan (VK) bands. The spectrum shown in Figure 9 is a composite of these three features. Four LBH sequences are indicated (Δv = 7, 8, 9,

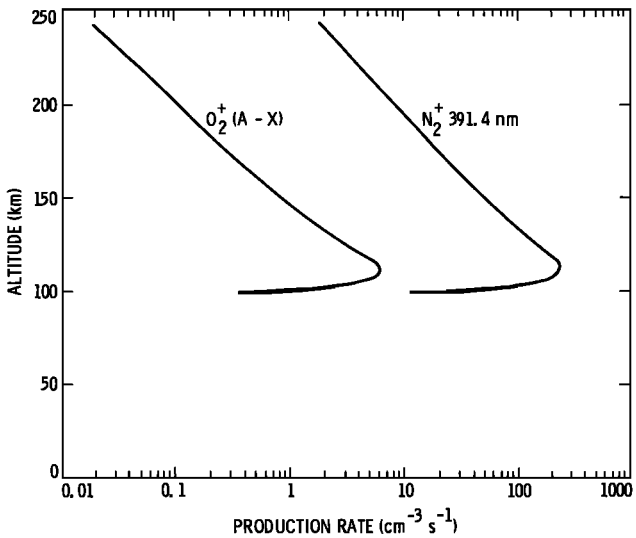

Fig. 8. Comparison of the production rates of N_2^+ (391.4 nm) and O_2^+ second negative bands as a function of altitude.

and 10) together with three of the prominent VK bands. Both the LBH [*Ajello and Shemansky*, 1985] and the O_2^+ bands are from our laboratory data. The VK are a theoretical calculation based upon the work of *Shemansky* [1969]. An O_2/N_2 ratio of 0.2 was assumed which is typical of the lower thermosphere. The relative intensities of these emissions were calculated using the Strickland model. However, because the VK system is not excited by direct electron impact and is severely quenched for $z < 150$ km, the scaling for this emission is only approximate. From Figure 9 it is clear that the O_2^+ second negative bands are likely to be overwhelmed by the more prominent N_2 emissions. In fact, the maximum contribution in any region of the spectrum is probably no more than 30%. However, *Beiting and Feldman* [1979] report high background counts present in their auroral data; the O_2^+ bands may be a contributor to this background.

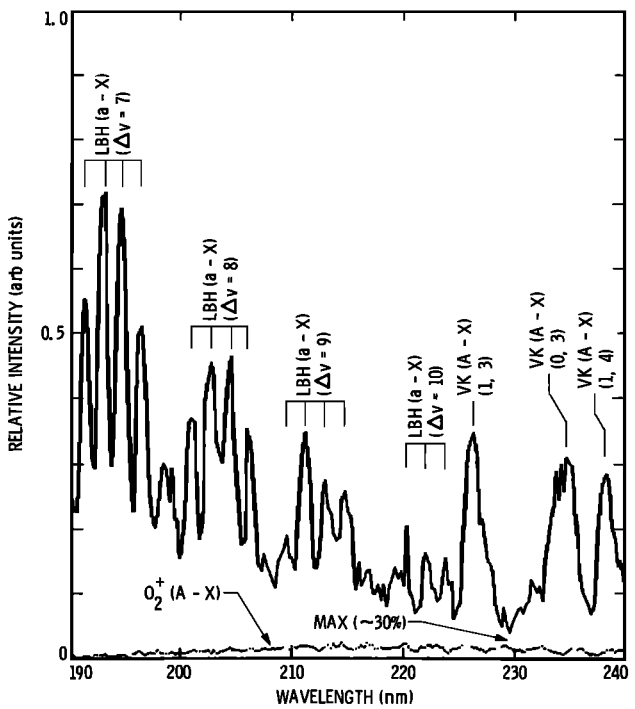

Fig. 9. Model auroral spectrum of O_2^+ (*A-X*), N_2 (LBH) and N_2 (VK) at 100 km. The scaled experimental spectrum of O_2^+ (*A-X*) is shown as a dotted line.

Acknowledgments. This work was supported by the Air Force Office of Scientific Research, the Aeronomy Program of the National Science Foundation grant ATM 8715709, and by NASA Planetary Sciences and Astronomy/Relativity Programs. We would like to acknowledge useful discussions with C. C. Lin and R. S. Schappe of the University of Wisconsin. G. K. James gratefully acknowledges the receipt of a National Research Council Resident Research Associateship award.

The Editor thanks M. D. Morrison and another referee for their assistance in evaluating this paper.

REFERENCES

Ajello, J. M., Emission cross sections of CO by electron impact in the interval 1260–5000 Å, I, *J. Chem. Phys.*, *55*, 3158, 1971*a*.

Ajello, J. M., Emission cross section of CO_2 by electron impact in the interval 1260–4500 Å, II, *J. Chem. Phys.*, *55*, 3169, 1971*b*.

Ajello, J. M., and B. Franklin, A study of the extreme ultraviolet spectrum of O_2 by electron impact, *J. Chem. Phys.*, *82*, 2519, 1985.

Ajello, J. M., and D. E. Shemansky, A reexamination of important N_2 cross sections by electron impact with application to the dayglow: The Lyman-Birge-Hopfield band system and N I (119.99 nm), *J. Geophys. Res.*, *90*, 9845, 1985.

Ajello, J. M., and S. K. Srivastava, UV studies of electron impact excitation of CS_2, *J. Chem. Phys.*, *75*, 4454, 1981.

Ajello, J. M., S. K. Srivastava, and Y. L. Yung, Laboratory studies of UV emissions of H_2 by electron impact: The Werner- and Lyman-band systems, *Phys. Rev. A*, *25*, 2485, 1982.

Ajello, J. M., D. Shemansky, T. L. Kwok, and Y. L. Yung, Studies of extreme-ultraviolet emission from Rydberg series of H_2 by electron impact, *Phys. Rev. A*, *29*, 636, 1984.

Ajello, J. M., et al., A simple ultraviolet calibration source with reference spectra and application to the Galileo orbiter ultraviolet spectrometer, *Appl. Opt.*, *27*, 890, 1988.

Beiting, B. E., and P. D. Feldman, Ultraviolet spectrum of the aurora (2000–2800 Å), *J. Geophys. Res.*, *84*, 1287, 1979.

Byrne, J., New bands in the second negative system of oxygen, *Proc. Phys. Soc. London*, *78*, 1074, 1961.

Chamberlain, J. W., *Physics of the Aurora and Airglow*, 195 pp., Academic, San Diego, Calif., 1961.

Coxon, J. A., and M. P. Haley, Rotational analysis of the $A\ ^2\Pi_u \rightarrow X^2\Pi_g$ second negative band system of O_2^+, *J. Mol. Spectrosc.*, *108*, 119, 1984.

Doolittle, P. H., R. I. Schoen, and K. E. Schubert, Dissociative photoionization of O_2, *J. Chem. Phys.*, *49*, 5108, 1968.

Edqvist, O., E. Lindholm, L. E. Selin, and L. Asbrink, On the photoelectron spectrum of O_2, *Phys. Scr.*, *1*, 25, 1970.

Erdman, P. W., and E. C. Zipf, Electron-impact of the O I λ1641.3 Å line emission, *Geophys. Res. Lett.*, *13*, 506, 1986*a*.

Erdman, P. W., and E. G. Zipf, Electron impact excitation of the O I λ 1172.6 Å multiplet, *Planet. Space. Sci.*, *34*, 1155, 1986*b*.

Erman, P., and M. Larsson, Lifetimes of excited levels in some important ion-molecules, part II, O_2^+, *Phys. Scr.*, *15*, 335, 1977.

Gattinger, R. L., and A. Vallance Jones, Quantitative spectroscopy of the aurora, II, The spectrum of medium intensity aurora between 4500 and 8900 Å, *Can. J. Phys.*, *52*, 2343, 1974.

Hedin, A. E., A revised thermospheric model based on mass spectrometer and incoherent scatter data: MSIS-83, *J. Geophys. Res.*, *88*, 10,170, 1983.

Hill, E., and J. H. Van Vleck, On the quantum mechanics of the rotational distortion of multiplets in molecular spectra, *Phys. Rev.*, *32*, 250, 1928.

Huber, K. P., and G. Herzberg, *Molecular Spectra and Molecular Structure*, vol. IV, *Constants of Diatomic Molecules*, Van Nostrand Reinhold, New York, 1979.

Huffman, R. E., F. J. LeBlanc, J. C. Larrabee, and D. E. Paulsen, Satellite vacuum ultraviolet airglow and auroral observations, *J. Geophys. Res.*, *85*, 2201, 1980.

Klotz, R., and S. D. Peyerimhoff, Theoretical study of the intensity of the spin- or dipole forbidden transitions between the $c^1\Sigma_u^-$,

$A'^3\Delta_u$, $A^3\Sigma_u^+$ and $X^3\Sigma_g^-$, $a^1\Delta_g$, $b^1\Sigma_g^+$ states in O_2, *Mol. Phys.*, *57*, 573, 1986.

Korol, V. I., S. M. Kishko, and V. V. Skubenich, Determination of excitation cross sections of some O_2^+ bands by the method of crossing beams, *Ukr. Fiz. Zh. Ukr. Ed.*, *13*, 1225, 1968.

Krupenie, P. H., The spectrum of molecular oxygen, *J. Phys. Chem. Ref. Data*, *1*, 423, 1972.

Lin, C. C., M. B. Schulman, R. S. Schappe, F. A. Sharpton, L. W. Anderson, W. A. M. Blumberg, and B. D. Green, Emission of radiation produced by electron beam excitation of oxygen gas, paper presented at 40th Gaseous Electronics Conference, Ga. Inst. of Technol., Atlanta, Ga., 1987.

McConkey, J. W., and J. M. Woolsey, Excitation of O_2^+ bands by electron impact, *J. Phys. B*, *2*, 529, 1969.

Pang, K. D., J. M. Ajello, B. Franklin, and D. E. Shemansky, Electron impact excitation cross section studies of methane and acetylene, *J. Chem. Phys.*, *86*, 2750, 1987.

Rapp, D., and P. Englander-Golden, Total cross sections for ionization and attachment in gases by electron impact, I, Positive ionization, *J. Chem. Phys.*, *43*, 1464, 1965.

Rees, M. H., and R. A. Jones, Time dependent studies of the aurora, II, Spectroscopic morphology, *Planet. Space Sci.*, *21*, 1213, 1973.

Saxon, R. P., and T. G. Slanger, Molecular oxygen absorption continua at 195–300 nm and O_2 radiative lifetimes, *J. Geophys. Res.*, *91*, 9877, 1986.

Shemansky, D. E., N_2 Vegard-Kaplan system in absorption, *J. Chem. Phys.*, *51*, 689, 1969.

Shemansky, D. E., J. M. Ajello, and D. T. Hall, Electron impact excitation of H_2: Rydberg band systems and the benchmark dissociative cross section for H Lyman-alpha, *Astrophys. J.*, *296*, 765, 1985.

Siskind, D. E., and C. A. Barth, Rocket observation of the N II 2143 Å emission in an aurora, *Geophys. Res. Lett.*, *14*, 479, 1987.

Srivastava, S. K., A. Chutjian, and S. Trajmar, Absolute elastic differential electron scattering cross sections in the intermediate energy region, I, H_2^*, *J. Chem. Phys.*, *63*, 2659, 1975.

Stewart, D. T., and E. Gabathuler, Some electron collision cross sections for nitrogen and oxygen, *Proc. Phys. Soc. London*, *72*, 287, 1958.

Strickland, D. J., J. R. Jasperse, and J. A. Whalen, Dependence of auroral FUV emissions on the incident electron spectrum and neutral atmosphere, *J. Geophys. Res.*, *88*, 8051, 1983.

Trajmar, S., and D. Register, Experimental techniques for cross-section measurements, in *Electron Molecule Collisions*, Chapter 6, edited by K. Takayanagi and I. Shimamura, p. 427, Plenum, New York, 1984.

Trajmar, S., W. Williams, and A. Kuppermann, Angular dependence of electron impact excitation cross sections of O_2, *J. Chem. Phys.*, *56*, 3759, 1972.

Wacks, M. E., Franck-Condon factors for the ionization of CO, NO, and O_2, *J. Chem. Phys.*, *41*, 930, 1964.

Wakiya, K., Differential and integral cross sections for the electron impact excitation of O_2, I, Optically allowed transitions from the ground state, *J. Phys. B*, *11*, 3913, 1978*a*.

Wakiya, K., Differential and integral cross sections for the electron impact excitation of O_2, II, Optically forbidden transitions from the ground state, *J. Phys. B*, *11*, 3931, 1978*b*.

Watson, C. E., V. A. Dulock, R. S. Stolarski, and A. E. S. Green, Electron impact cross sections for atmospheric species, *J. Geophys. Res.*, *72*, 3961, 1967.

Yoshino, K., and Y. Tanaka, Rydberg absorption series and ionization energies of the oxygen molecule, I, *J. Chem. Phys.*, *48*, 4859, 1968.

J. M. Ajello, B. Franklin, and G. K. James, Jet Propulsion Laboratory, California Institute of Technology, 4800 Oak Grove Drive, Mail Stop 183-601, Pasadena, CA 91109.

D. E. Shemansky, Lunar and Planetary Laboratory, University of Arizona, Tucson, AZ 85721.

D. Siskind, Laboratory for Atmospheric and Space Physics, University of Colorado, Boulder, CO 80302.

T. G. Slanger, Chemical Physics Laboratory, SRI International, Menlo Park, CA 94025.

(Received January 26, 1988;
revised March 31, 1988;
accepted April 5, 1988.)